



## Sequence analysis

# AttCRISPR : a spacetime interpretable model for prediction of sgRNA on-target activity

Liming Xiao<sup>1</sup>, Yunqi Wan<sup>1</sup> and Zhenran Jiang<sup>1,\*</sup>

<sup>1</sup>Department of Computer Science & Technology, East China Normal University, Shanghai, 200062, China.

\*To whom correspondence should be addressed.

Associate Editor: XXXXXXXX

Received on XXXXX; revised on XXXXX; accepted on XXXXX

### Abstract

**Motivation:** More and more higher specificities Cas9 variants are developed to avoid the off-target effect, which bring a significant volume of experimental data. Conventional machine learning performance poorly on these datasets, while model based on deep learning are often lack of interpretability, which makes it difficult for researchers to understand its decisions, not to mention to design high-activity sgRNA with the insights brought by the model. Moreover, neither the deep learning based model with existing structure can not satisfy enough precision at such huge datasets.

**Results:** To overcome these, we design and implement AttCRISPR, a intrinsic interpretable method based on deep learning to predict the on-target activity. In this paper, we find that based on the preprocessing of the input base sequence, the deep learning models can be divided into two categories, methods in spatial domain with the input of encoded base sequence and in temporal domain with the input of embedded base sequence. Based on the categorization above, we assume that spatial and temporal method are heterogeneous, and use a full connection layer to stack them, which achieve a better performance. Our model was trained and tested on the biggest dataset, the same dataset as DeepHF used, as far as we know for performance evaluation. In addition, benefits from two attention modules, spatial and temporal attention modules, AttCRISPR has strong interpretability. Through them, we can understand the decisions made by AttCRISPR at both global and local levels without other post hoc explanations techniques. Further, interpretability can be used to help us design and optimize sgRNA activity without exhaustively search. AttCRISPR can compete with state-of-the-art method in these datasets, and achieves an average spearman value of 0.872, 0.867, 0.867 (corresponding to WT-SpCas9, eSpCas9(1.1), SpCas9-HF1) under tenfold shuffled validation.

**Availability:** The example code are available at <https://github.com/South-Walker/AttCRISPR>

**Contact:** xlm@xiaoliming96.com

**Supplementary information:** Supplementary data are available at *Bioinformatics* online.

## 1 Introduction

Clustered regularly interspaced short palindromic repeats (CRISPR) / CRISPR associated protein 9 (Cas9) systems is preferred over other biological research and human medicine technologies now, because of its efficiency, robustness and programmability. Cas9 nucleases can be directed by short guide RNAs (sgRNAs) to introduce site-specific DNA double-stranded breaks in target, so to enable editing site-specific within the mammalian genome (Jinek *et al.*, 2012; Cong *et al.*, 2013; Mali *et al.*,

2013). CRISPR/Cas9, to a large extent, has developed genetic therapies at the cellular level, while there are still severe medical disadvantage even now which has greatly hindered the further clinical application of the CRISPR/Cas9 systems. One of these disadvantage is due to point mutations caused by off-target effects (Rubeis and Steger, 2018; Kang *et al.*, 2016; Ishii, 2017; Liang *et al.*, 2015). To overcome this disadvantage, a solution is to engineer CRISPR / Cas9 with higher specificities. That's why more and more higher specificities Cas9 variants, such as enhanced SpCas9 (eSpCas9(1.1)), Cas9-High Fidelity (SpCas9-HF1) (Ishii, 2017; Slaymaker *et al.*, 2016), hyper-accurate Cas9 (HypaCas9) (Kleinstiver *et al.*, 2016), been developed and bring a significant volume

of experimental data, that is to say researchers have to face the difficulty of analyzing such huge and heterogeneous data.

The activity of chosen sgRNA sequence determines the success of genome editing, however distinctly fluctuant behaviors have been observed for the performance of different sgRNAs, even in the same Cas9 system. Some optimum sgRNAs can hit almost all targets alleles, while another don't even show activity (Wang *et al.*, 2019). This fact indicates that it's meaningful to explore an efficient approaches to predict sgRNA activity and even guide sgRNA design.

In practice, there have been a number of application and toolkit applied in this task. In the earlier studies, methods in silico are categorized into three types: (1) alignment-based, (2) hypothesis-driven and (3) learning-based (Chuai *et al.*, 2018). Recently we noticed that the last type of method seems to be getting more attention because of huger and huger data set (Liu *et al.*, 2019a).

Learning-based method, which designed to predict the on-target activity (or off-target probability) of sgRNAs, is essentially a computational model built by machine learning algorithm, not only conventional machine learning but also deep learning algorithm. In general, the single or multiple base sequences (vary according to the task) and biological features are represented as a multi-dimensional vector  $X \in \mathbb{R}^d$ , and  $d = l + b$ , where  $l$  refers to the length of base sequences and  $b$  refers to the number of biological features, these methods can be represented as

$$y = \text{Score}(X) \quad (1)$$

where  $\text{Score}(\cdot)$  depends on the algorithm being selected, and  $y$  denotes the predicted value. Some studies on HT\_ABE and HT\_CBE have shown that deep learning based models often outperformed conventional machine learning, when the number of sgRNAs in the data set reached a certain level (Song *et al.*, 2020; Kim *et al.*, 2018, 2019). Per contra, conventional machine learning algorithms, such as linear regression, logistic regression and the decision tree, are often more interpretable due to the fewer parameters and clearer mathematical assumptions. In short, what was needed for developer is to trade-off accuracy and interpretability. Muhammad Rafid *et al.* consider deep-learning models as black boxes and believe they lack interpretability, motivated by the empirical assertion, they turn to build a model based conventional machine learning to compete with state-of-the-art deep learning models (Muhammad Rafid *et al.*, 2020). On the other hand, input perturbation based feature importance analysis become a preferred components to reveal the importance of features in deep learning models. Liu *et al.* use a sliding window of length 2 to extract dimeric as input and rank the position of dimeric by contribution to final output (Liu *et al.*, 2019b). One regret is that subject to the processing of the input sgRNA sequence, their analysis can not exactly on the nucleotide class. Further, SHAP, one of the most prominent of model explain techniques, has been widely used to understand the decision made by the model. Wang *et al.* develop DeepHF, a deep learning based model, and use Deep SHAP to revealed nucleotide contributions (Wang *et al.*, 2019). Deep SHAP is a compositional approximation of SHAP values since it is challenged to compute SHAP values exactly, especially for a complex deep neural networks. In our understanding, the method based on input perturbation often requires better generalization ability of the model (even for artificial ridiculous noise data).

Beyond that, existing analysis of the models interpretability are all at global level, and result is a general pattern in the datasets. For example, which position has a great impact on the final decision of the model and which position-dependent nucleotide has a positive impact on the activity. Lack of analysis at local level. For example, which structure causes the low activity of a certain nucleotide sequence and how to improve its activity with a few modification. In light of the above, we believe it is essential to develop a model which can not only match deep learning based model in

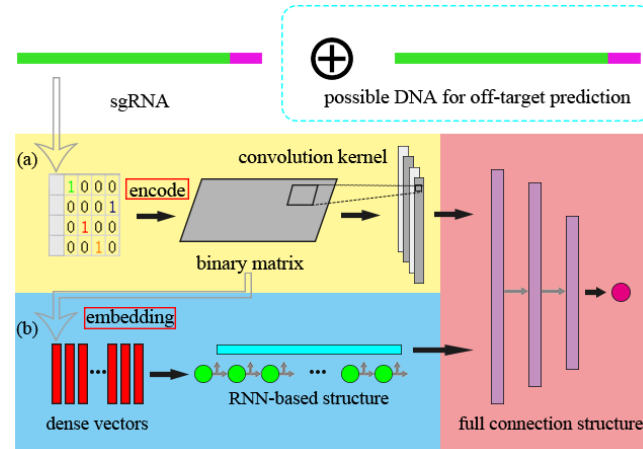


**Fig. 1.** Two categories of the deep learning models used in sgRNA related task. (a) Model work in spatial domain. In spatial domain, the base sequence is encoded into a binary matrix (or a binary image). Since convolution has great advantages in extracting spatial features, the convolutional neural network is an excellent tool in spatial domain. (b) Model work in temporal domain. In temporal domain, the base sequence (represented by the binary matrix) is embedded into a sequence of high-dimensional vector, in which the recurrent neural network perform better. In addition, we note that the last layers of neural network are usually full connection structure (not necessarily), which greatly increases the difficulty of understanding the decisions of model.

performance, but also with strong interpretability that can be comparable to conventional machine learning method.

Deep neural network has shown its power in the study of CRISPR/Cas9 and its improved Systems (Liu *et al.*, 2019a). Most of the deep neural network existing are the combination of recurrent neural network (RNN), convolutional neural network (CNN), fully connected neural network (FNN), and their variants. As Figure 1 show, We found that the deep learning models used in sgRNA on-target activity (even for off-target effect) prediction tasks in recent years can be divided into the following two categories according to the encoding approach of the sgRNA sequence (sgRNA-DNA sequence pair, for off-target effect prediction):

1. Methods in spatial domain. Some previous studies have used model based CNN to predict gRNA on-target activity or off-target effects (Lin and Wong, 2018; Kim *et al.*, 2018; Chuai *et al.*, 2018). They process sgRNA base sequence inputs with the help of one-hot encoding idea. In other words, they regard it as two-dimensional image data, and use convolution layer to extract potential features in spatial domain. It is worth noting that Zhang *et al.* adds bidirectional gated recurrent unit (BGRU, in short), a RNN variant, after pooling layer of classic CNN network (Zhang *et al.*, 2020). Our explanation is that BGRU assists CNN to extract spatial features in one dimension, under this belief it belong to this category.
2. Methods in temporal domain. Although RNN-based network have been shown effective to improve the performance of the model with temporal sequential input, especially in natural language processing and sequential recommendation, RNN be not used for gRNA activity prediction, until recently (Wang *et al.*, 2019; Liu *et al.*, 2020, 2019b). They consider the nucleotides (can also dimer or polymer) in the sgRNA sequence as word, and the sgRNA sequence itself as a sentence (from 5' to 3'), then a trainable matrix (could be either supervised or unsupervised) is used to project the word to the dense real-valued space. This technology is called embedding, which generates the base embedding. RNN further encoding the base embedding into a sequence of hidden state vector. Specially, Liu *et al.* use RNN

and CNN in parallel to extract features in base embedding (Liu *et al.*, 2019b). However, base embedding is not spatially interpretable (different from one-hot encode), and they have no way to further explore the correlation between CNN and RNN output. Almost all RNN based models used in sgRNA on-target activity or off-target effect flatten the hidden state vector into a one-dimensional vector as the input of the fully connected layer. It is a pity that the temporal sequential dependency of hidden state vector are rarely noticed. To summarise, RNN has limited representation power in capturing spatial feature. Furthermore, hidden state vector representation is usually hard to understand and explain.

Attention mechanism has demonstrated its power in Natural Language Processing, Statistical Learning, Speech and Computer Vision. It makes model tends to focus selectively on parts of the input which is help in performing the task effectively. Previous observation have shown that Cas9 preferentially binds sgRNAs containing purines but not pyrimidines (Wang *et al.*, 2014) and multiple thymine in the spacer impairing sgRNA activity (Wu *et al.*, 2014), that is to say some specific nucleotide and base position need more attention compared to others. The above is the premise of introducing attention mechanism. Strictly speaking, we are not the first to bring attention mechanisms into this field. The most similar approach to ours is the work based on transformer by Liu *et al.*. They use transformer, a components based on attention mechanism, instead of RNN to improve the ability of temporal feature extraction, hence, enhance the performance of their model (Liu *et al.*, 2019b; Vaswani *et al.*, 2017). In our work, the interpretability benefit from attention mechanism is more focused. In this paper, our main contributions are as follows:

- Present a novel deep-learning model, which can extract potential feature representation of sgRNA sequence in both spatial and temporal domain parallelly. Finally, the ensemble learning method is used to combine the two to achieve better performance than other models. It doesn't belong to any of the above categories of existing approaches.
- Introduce attention mechanism into our model. As a result, It does not need post hoc explanations techniques based on input perturbation to explain itself. It is intrinsic interpretable in both temporal and spatial domains. In the spatial domain it's at global level, while at local level in the temporal domain. Thus, it is transformed from a black box to an intrinsically interpretable model with the performance of deep learning based model.
- Through ablation analysis and testing a series of possible network structure, we find there are multiple components and strategy can improve the performance of our model and constructed AttCRISPR, which could outperform the current state-of-the-art tool on DeepHF dataset.

## 2 Materials and methods

### 2.1 Sequence encoding and embedding

For encoding process, we use the complementary base to represent the original base in sgRNA, as others do. Further, we use one-hot encode strategy, which's is to say, we encoding each base in sgRNA into a four-dimensional vector (encode A,T,G,C into [1,0,0,0], [0,1,0,0], [0,0,1,0], [0,0,0,1], respectively), called one-hot vector. Then a sgRNA can be considered as a matrix  $X_{oh} \in \mathbb{R}^{l \times 4}$ , named one-hot matrix (a little sparse, since an one-hot vector is zero in all but one dimension). We believe it is meaningful to regard  $X_{oh}$  as a binary image, therefore, it is used as an input of convolutional neural network, which performs well in the image field. Meanwhile, as mentioned above, one-hot matrix is a little sparse.

To facilitate the training process, we can mapping each one-hot vector into a dense real-valued high-dimensional space, which is called embedding. Concretely speaking, at the matrix level, the formula is as follows

$$X_e = X_{oh} E_m \quad (2)$$

where  $X_e$  named embedding matrix,  $E_m \in \mathbb{R}^{4 \times m}$  is a trainable transformational matrix,  $m$  refers to the dimension of embedding space. We believe it is also meaningful to regard nucleotides in the sgRNA sequence as word, and the sgRNA sequence itself as a sentence, Guided by this belief  $E_m$  is the word embedding matrix and  $X_e$  is the sentence embedding in natural language processing (NLP). Therefore,  $X_e$  is used as an input of recurrent neural network (or its variant), which performs well in the NLP field. In the area of NLP, there have been many methods based on pre-training and unsupervised learning been developed to determine the  $E_m$ . However, we believe that sgRNA sequence is not a natural language in the true sense, the method above does not apply to it. So  $E_m$  will be trained along with the model as a whole.

Due to each element of  $X_{oh}$  is interpretable (representing whether there is a corresponding nucleotide type at the corresponding location), we call  $X_{oh}$  the spatial input, and the convolutional neural network work on  $X_{oh}$  is method in spatial domain. In other hand, different from  $X_{oh}$ ,  $X_e$  can only be explained in the first dimension (representing the embedding vector of corresponding nucleotide type), and embedding vector is difficult for humans to understand. That's why we call  $X_e$  the temporal input, and the recurrent neural network (or its variant) work on  $X_e$  is method in temporal domain.

### 2.2 Neural network architecture

Based on the categorization above, we assume that method in spatial domain and in temporal domain are heterogeneous, which can satisfy the diversity premise of ensemble learning. Based on assumption above and ensemble learning, we follow the stacking strategy to develop AttCRISPR which can extract potential feature representation of sgRNA sequence in both spatial and temporal domain parallelly. Further, we apply attention mechanisms in both spatial and temporal domain respectively to enhance the interpretability of AttCRISPR.

#### 2.2.1 First-order preference and second-order preference

Before introducing the neural network architecture of AttCRISPR, Let's define first-order preference and second-order preference for convenience. Taking a simple linear regression model as an example, for input  $X$  in Equation (1),  $y$  in Equation (1) is as following

$$y = AX \quad (3)$$

where  $A \in \mathbb{R}^d$ , the total differential of  $y$  in Equation (3) is as following

$$dy = \sum_i^d A_i dX_i \quad (4)$$

where  $A_i$  and  $X_i$  denotes the  $i$ -th dimension of the vector  $X$  and  $A$ ,  $A_i$  indicates how dramatically the function changes as  $X_i$  changes in a neighborhood of  $X$ , in other word, the importance of  $X_i$ . That's why we'll call  $A$  first-order preference in our paper. Specifically, we use a vector  $A_i$  to build the first-order original preference at position  $i$  within sgRNA sequence, and  $X_i$  is an embeddedness of the  $i$ -th feature, then  $A$  and  $X$  are two matrix. Further, the final result can be weighted by a trainable non-negative weight vector  $W \in \mathbb{R}^l$ , as follow

$$y = W \cdot AX^T \quad (5)$$

then we define  $\tilde{A}$  as the first-order combine preference matrix (or just first-order preference), which means  $\tilde{A}$  can be expressed linearly by  $A$  as

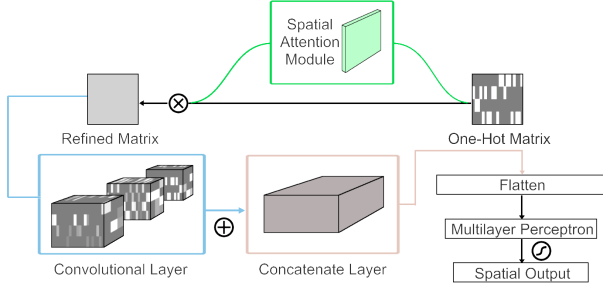


**Fig. 2.** The architecture of spatial domain method in AttCRISPR. The input of the method is encoded sgRNA sequence  $X_{oh}$ , a  $21 \times 4$  one-hot matrix. Then refine it through a spatial attention module, which could tell us the importance of a specific matrix element (or just say, pixel). A simple convolutional neural network followed is applied to extract potential feature representation of sgRNA sequence. In the last step, we flatten the output of convolutional neural network into a one dimensional vector and use a multilayer perceptron with sigmoid activation function to achieve the spatial output  $y_s$ .

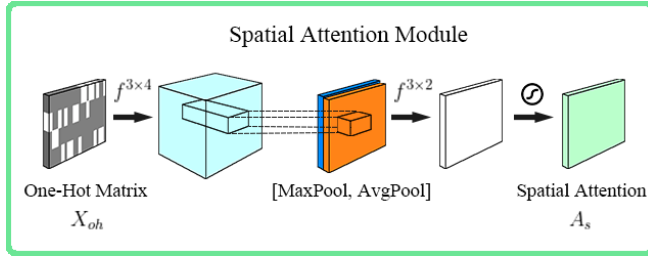


**Fig. 3.** Details of spatial attention module. A convolution layer is used to generate multi-channel map from  $X_{oh}$ . Then concatenated the output of both max-pooling and average-pooling method and forward it to the last convolution layer. A sigmoid function is used to map the final result to a range of zero to one at last, which generates the spatial first-order preference matrix  $A_s$ .

follow

$$\tilde{A} = BA \quad (6)$$

where the weight matrix  $B \in \mathbb{R}^{l \times l}$  is learned through attention mechanism, which we'll call the second-order preference matrix in our paper due to its calculation is based on first-order preference, it can explain how a particular pattern containing two nucleotides affects the base sequence. Then the predicted value can be expressed as

$$y = W \cdot \tilde{A} X_e^T \quad (7)$$

### 2.2.2 Method and attention in spatial domain

As Figure 2 show, method in spatial domain relies on the convolutional neural network. As previously mentioned, sgRNA sequence has been encoded into a  $21 \times 4$  one-hot matrix  $X_{oh}$ , and we regard  $X_{oh}$  as a binary image. Then, convolution kernels with different size are used to extract potential spatial features just like what other do in computer vision. According to the foregoing, the Spatial Attention Module proposed by Woo *et al.* can be applied in our method in spatial domain, which was used to improve the performance of CNN in vision tasks.

As Figure 3 show, Given an one-hot map  $X_{oh}$ , spatial attention module generating spatial attention matrix  $A_s \in \mathbb{R}^{l \times 4}$  with the same as  $X_{oh}$  in shape. Each element of  $A_s$  is constrained to a range of zero to one, implemented by a sigmoid function, which reflects the importance of the corresponding elements of  $X_{oh}$ . The overall spatial attention process can

be summarized as:

$$\begin{cases} X_{mc} = f^{3 \times 4}(X_{oh}) \\ A_s = \sigma(f^{3 \times 2}([AvgPool(X_{mc}); MaxPool(X_{mc})])) \\ X_{rf} = A_s \otimes X_{oh} \end{cases} \quad (8)$$

where  $f^{p \times q}$  represents a convolution operation with the filter size of  $p \times q$ ,  $p, q \in \mathbb{Z}^+$ ,  $X_{mc}$  is a multi-channel map generated by  $X_{oh}$ ,  $\sigma$  denotes the sigmoid function, AvgPool denotes the average-pooling operation, MaxPool denotes the max-pooling operation,  $\otimes$  denotes element-wise multiplication. Spatial attention matrix  $A_s$  formally conforms to our proposed definition of first-order preference (each element of  $X_{oh}$  is multiplied by the corresponding element of  $A_s$ ), in other word, element of  $A_s$  reveal how important the corresponding elements in  $X_{oh}$  is. We think it can reveal the preference of the scoring function at each position. For instance, follow the encoding rules above, train spatial domain part of AttCRISPR with the WT-SpCas9 dataset. Then take the average of all spatial attention matrix, and the element in the first row and third column are closer to 1, which means when calculate the final score, G typically may have a important contribution at first position within sgRNA sequence. In fact, this corresponds to some early studies concerning the Human (hU6) promoter, which is believed to require G as the first nucleotide of its transcript (Cong *et al.*, 2013; Jinek *et al.*, 2012; Mali *et al.*, 2013).

### 2.2.3 Method and attention in temporal domain

As Figure 4 show, temporal domain part of AttCRISPR relies on the recurrent neural network (or its variant). As previously mentioned, we mapping each one-hot vector into a dense real-valued high-dimensional space follow the Equation (2), which generates the embedded matrix  $X_e$ . And we regard  $X_e$  as a sequential data, or temporal data. Recurrent neural network (or its variant) has showed outstanding performance in the tasks with temporal data (for instance, natural language processing, sequential recommendation). That's why we prefer to use it to extract potential temporal features. To be precise, we prefer the architecture of encoder-decoder which has been proven to be effective in Seq2Seq task. Two main differences we have to face are that sgRNA is not a natural language in the traditional sense, and we don't have to translate it to other sequence. To accommodate them, the embedded matrix  $X_e$  is used as input of both the encoder and decoder, and the sequence of decoder is to build the first-order preference of sgRNA sequence  $\tilde{A}$ . As mentioned above, the predicted value  $y$  should satisfy Equation (7).

On this basis, we apply the idea of attention mechanism which has been widely used in natural language processing tasks to AttCRISPR in the method of temporal domain, and name it Temporal Attention Module (Vaswani *et al.*, 2017; Luong *et al.*, 2015). As the idea of Vaswani *et al.*, Temporal Attention Module satisfies the following equation

$$Attention(Q, K, V) = align(Q, K)V \quad (9)$$

where the  $align(\cdot)$  is put forward by Luong *et al.*  $Q, K, V$  are queries, keys and values matrix accordingly in the paper of Vaswani *et al.*

As Figure 5 show, in our attention module they are calculated by the following equation

$$\begin{cases} K_i = Encoder(X_{e_i}, \theta_E, K_{i-1}) \\ Q_i = Decoder(X_{e_i}, \theta_D, Q_{i-1}) \\ V = K \end{cases} \quad (10)$$

where vector  $K_i, Q_i$  denotes the  $i$ -th row of the matrix  $K$  and  $Q$  accordingly,  $Encoder(\cdot)$  and  $Decoder(\cdot)$  are independent GRU units,  $\theta_E$  and  $\theta_D$  denote all the related parameters of GRU networks accordingly. In the actual implementation, we apply the bidirectional GRU networks

for better performance, and for the sake of conciseness, we show a conventional GRU network here. The function  $align(\cdot)$  is as follows

$$B = align(Q, K) \quad (11)$$

$$B_i = softmax(Q_i K^T) \otimes G_i \quad (12)$$

$$G_{ij} = \begin{cases} exp(\frac{(i-j)^2}{-2\sigma}) & , |i-j| \leq \sigma \\ 0 & , |i-j| > \sigma \end{cases} \quad (13)$$

where the matrix  $B \in \mathbb{R}^{l \times l}$  is the second-order preference we need, and vector  $B_i$  denotes the  $i$ -th row of the matrix  $B$ .  $G \in \mathbb{R}^{l \times l}$  is the damping matrix base on Gaussian function. Since a simple belief that the closer the base is to the  $i$ -th position, the more it affects the  $i$ -th position normally, we use the damping matrix  $G$  to constrain the network learning.  $\sigma$  represents a threshold of length, any base over this length from the position  $i$  is not considered to be affected. Further, if we think of the values matrix as a vector form of the first-order preference  $A$  in Equation (6), we can reach the following equation

$$\tilde{A} = BV \quad (14)$$

according to above, values matrix  $V$  comes from the hidden states of a bidirectional GRU networks, which is usually hard to understand and explain. While  $B$  is the second-order preference matrix obtained by the attention mechanism, in our belief, the  $j$ -th dimension of  $B_i$ , denoted as  $B_{ij}$ , can reveal the effect of the base at position  $j$  on position  $i$  in the biological sense.

#### 2.2.4 Model ensemble following stacking strategy

As Wang *et al.*; Wang *et al.* have shown, some indirect sgRNA features, which can't be obtained directly by deep learning, including position accessibilities of secondary structure, stem-loop of secondary structure, melting temperature, and GC content are strongly associated with sgRNA activity. It's worth noting that in the work of Wang *et al.*, hand-crafted biological features didn't be normalized. Since the wide range of data distribution, we believe it makes sense to normalize it, and we preprocess they based on the standard score (Z-Score).

Then we use a simple full connection network to extract the indirect features, and call the output of fully connection network  $y_{bio}$ . As mentioned above, we assume that method in spatial domain and in temporal domain are heterogeneous, which can satisfy the diversity premise of ensemble learning. That's why we follow the stacking strategy, integrate the methods in time domain and space domain. Specifically, the  $y_{bio}$ , the spatial output  $y_s$  and the temporal output  $y_t$  we got earlier are concatenated and then weighted averaging is performed through a full connection layer as follow

$$y = W[y_{bio}; y_s; y_t] \quad (15)$$

where,  $y$  is the final prediction value of AttCRISPR,  $W$  is the weight learned by the full connection network. In the actual implementation, we freeze the network in the spatial domain and temporal domain at first, in order to make our network focused on learning the weight  $W$ . Later in the process, in the fine tuning of AttCRISPR, the parameters of the entire network are adjusted.

### 2.3 Datasets and current prediction method

The dataset we used for training, validation and testing is built by Wang *et al.* (Wang *et al.*, 2019). We extracted 55604, 58617, 56888 sgRNAs with activity (represented by insertion/deletion (indel)) for WT-SpCas9, eSpCas9(1.1) and SpCas9-HF1 respectively, from its source data. As far as we know, the best performance on this dataset is the DeepHF of Wang *et al.* currently, which base on deep learning and bidirectional LSTM architecture. DeepHF achieved Spearman correlation coefficients

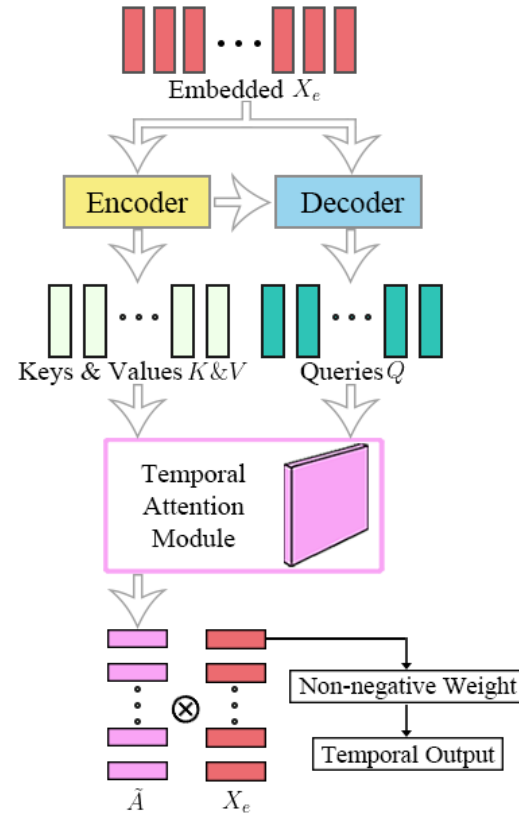


**Fig. 4.** The architecture of temporal domain method in AttCRISPR. The input of the method is embedding sgRNA sequence  $X_e$ , a  $21 \times e$  embedding matrix, where  $e$  is the dimension of a nucleotide embedding vector. Then Keys  $K$ , Values  $V$  and Queries  $Q$  is generated through a classic encoder-decoder structure which is need for temporal attention module. Next, the temporal attention module generates the first-order preference  $\tilde{A}$ , a  $21 \times e$  matrix (or a vector set). Each of the row vectors in matrix  $\tilde{A}$  represents the base preference of sgRNA at the corresponding position, we use their dot product with the corresponding row vector in embedded  $X_e$  to build the score of corresponding position. Hence, a full connection layer is used to weighted average them and achieve the temporal output  $y_t$ .

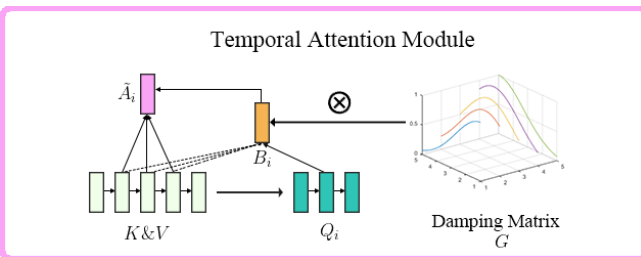


**Fig. 5.** Details of temporal attention module. To generate the first order preference vector in the  $i$  position of sgRNA  $\tilde{A}_i$ . First, the  $i$ -th row vector of the queries matrix  $Q_i$  is multiplied by the transpose of the keys matrix  $K^T$ , and apply a softmax function to obtain a preliminary weights vector on the values. Second, to favor the alignment points near  $i$ , the weights vector obtained is multiplied element-by-element by the  $i$ -th row vector of the damping matrix  $G$ , as Equation (12) has shown.  $G_{ij}$  can be regarded as the result of place a Gaussian distribution centered around  $i$ , then sampling the position  $j$  (a scaling factor is used to ensure the sum of  $G_i$  is 1). Then we achieve the second-order preference matrix  $B$ , it is also a weights matrix on the values. So the first-order preference matrix  $\tilde{A}$  come from the product of  $B$  and values matrix  $V$ . Although it's not shown above, it is also worth noting that, a full connection layer with L2 constraints is used to generates a transformation matrix in order to ensure  $\tilde{A}_i$  and  $X_{e_i}$  are in the same vector space. Temporal attention module generates the temporal first-order preference matrix  $\tilde{A}$  and the temporal second-order preference matrix  $B$ .



Table 1. The methods compared in our work and brief description of these methods

Method	Neural	End2end	Description
CNN*	Yes	Yes	Naive convolutional neural network
RNN*	Yes	Yes	Bidirectional long short-term memory neural network
XGBoost*	No	Yes	Extreme Gradient Boosting regression tree
MLP*	Yes	Yes	Multilayer perceptron
DeepHF*	Yes	No	Bidirectional long short-term memory neural network (with hand-crafted biological features)
CRISPRpred(SEQ) <sup>#</sup>	No	No	A conventional machine learning pipeline
SpAC	Yes	Yes	Spatial AttCRISPR
TAC	Yes	Yes	Temporal AttCRISPR
EnAC	Yes	Yes	Ensemble AttCRISPR (without hand-crafted biological features)
StAC	Yes	No	Standard AttCRISPR

Note: The method with superscript of \* and <sup>#</sup> is reported by Wang *et al.* and Muhammad Rafid *et al.* respectively. Specially, CRISPRpred(SEQ) take another set of hand-crafted sequence-based feature to improve performance.

of 0.867, 0.862 and 0.860 for WT-SpCas9, eSpCas9(1.1) and SpCas9-HF1 respectively.

Another tool worth noting is CRISPRpred(SEQ), which is based on conventional machine learning and need complicated human feature engineering exercise (Muhammad Rafid *et al.*, 2020). They also test their tool with this dataset and achieved Spearman correlation coefficients of 0.838, 0.830 and 0.821 for WT-SpCas9, eSpCas9(1.1) and SpCas9-HF1 respectively (without any hyperparameter tuning).

Wang *et al.* implemente a tenfold shuffled validation to evaluate the stability of the performance of DeepHF. To be more specific, each set is shuffled and divided into three parts, 76.5%, 15% and 8.5% of the relevant data was used as the training, test and validation set respectively in a single experiment. The experiment is repeated ten times with the results recorded and averaged finally. In order to make the comparison apples to apples, we will follow this strategy to design experiments.

2.4 Experiments

Two different sets of experiments are carried out in our work. The first one is designed for ablation analysis of AttCRISPR. We compare the performance of end2end method (without any hand-crafted biological features) in both spatial and temporal domain. Furthermore, we test the ensemble method based on the same strategy, which proved that the ensemble of method in both spatial and temporal domain can significantly improve the performance.

The second experiment is designed to compare the performance of AttCRISPR and other current prediction method. In order to make the comparison apples to apples, we reduce the dimensionality of the same hand-crafted biological features as DeepHF's, which has been shown to enhance the predictability of a deep-learning model greatly, with a multilayer perceptron. Then follow the Equation (15) to achieve the final prediction value. AttCRISPR (with the hand-crafted biological features) performs better on all three data sets than DeepHF, the current state-of-the-art.

Our baselines have a comprehensive coverage of the methods tested in these datasets. In Table 1, we annotate some properties of these baselines

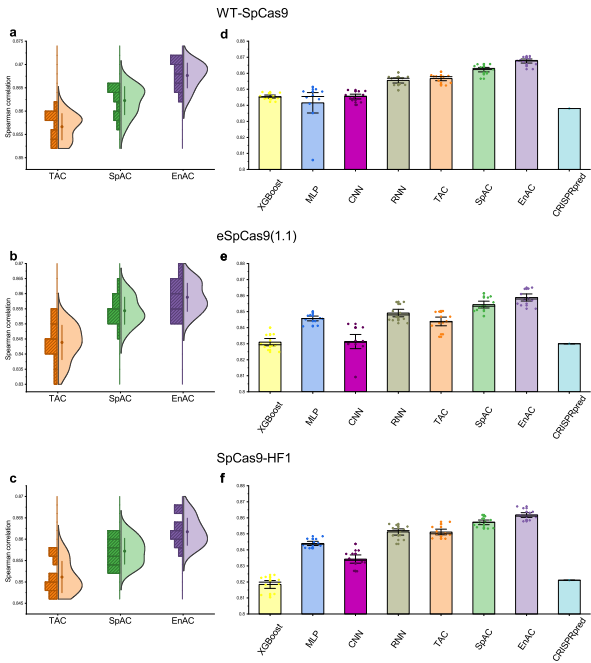


Fig. 6. In the absence of hand-crafted biological features, performance of different algorithms for sgRNA activity prediction. (a)-(c) The performance of Temporal AttCRISPR, Spatial AttCRISPR and Ensemble AttCRISPR. The half-violin plots show the mean and distribution of the Spearman correlation coefficient between predicted and measured sgRNA activity scores over all tests. (d)-(f) In the absence of hand-crafted biological features, the performance of all prediction methods in these datasets as far as we know. The *mean*  $\pm$  *s.d.* of the Spearman correlation coefficient between predicted and measured sgRNA activity scores are shown in the bar plots.

(is/isn't neural models, is/isn't end2end models) All the experiments were carried out in Python 3.6 using Keras 2.2.4 and one GeForce RTX 2080Ti Super was used for training and testing if needed.

3 Results

We designed experiments to address the following questions:

- In the absence of hand-crafted biological features, whether the stacking of method in spatial domain and temporal domain can get better performance then use these method alone?  $\rightarrow$  Section 3.1
- How does AttCRISPR perform compared to current state-of-the-art methods, covering both conventional machine learning and deep-learning models?  $\rightarrow$  Section 3.2
- How can researcher understand the decisions make by AttCRISPR locally and globally, based on attention mechanisms?  $\rightarrow$  Section 3.3

3.1 Model building and stacking

In Table 2, we list the performance of methods in spatial or temporal domain and the stacking of methods. Temporal AttCRISPR, TAC for short, achieved Spearman correlation coefficients of 0.857, 0.844, 0.851 in above three dataset. Spatial AttCRISPR, SpAC for short, corresponds to 0.862, 0.854, 0.857. In the absence of hand-crafted biological features. Ensemble AttCRISPR achieve the best performance of our knowledge, corresponds to 0.868, 0.859, 0.862.

In addition, in Table 2, the performance of other methods without using hand-crafted biological features, are also recorded. Regardless of the method we developed, RNN reported by Wang *et al.*, which can be

Table 2. Performance comparisons for different methods in the absence of hand-crafted biological features (take Spearman correlation coefficient as evaluation index)

Method	WT-SpCas9	eSpCas9(1.1)	SpCas9-HF1
XGBoost*	0.845	0.831	0.818
MLP*	0.842	0.846	0.844
CNN*	0.846	0.831	0.834
RNN*	0.856	0.849	0.851
TAC	0.857	0.844	0.851
SpAC	0.862	0.854	0.857
EnAC	<b>0.868</b>	<b>0.859</b>	<b>0.862</b>
CRISPRpred(SEQ) <sup>#</sup>	0.838	0.830	0.821

Table 3. Performance comparisons for methods before and after integrating with hand-crafted biological features (take Spearman correlation coefficient as evaluation index)

Method	WT-SpCas9		eSpCas9(1.1)		SpCas9-HF	
	Mean	Std Dev ( $\times 10^{-3}$ )	Mean	Std Dev ( $\times 10^{-3}$ )	Mean	Std Dev ( $\times 10^{-3}$ )
RNN*	0.856	3.33	0.849	5.00	0.851	4.11
EnAC	0.868	2.66	0.859	4.66	0.862	3.19
DeepHF*	0.867	<b>2.37</b>	0.862	4.24	0.860	3.21
StAC	<b>0.872</b>	2.55	<b>0.867</b>	<b>3.71</b>	<b>0.867</b>	<b>2.65</b>

Note: The method with superscript of \* and <sup>#</sup> is reported by Wang *et al.* and Muhammad Rafid *et al.* respectively. In the tables, we use the results reported in the relevant paper as the performance of the method directly.

categorized as the method in temporal domain, is the most predictive with Spearman correlation coefficients of 0.856, 0.849, 0.851. It’s obvious that the ensemble AttCRISPR is better at prediction (Figure 6 a-c). Furthermore, the prediction ability of models could be boosted by addition of other hand-crafted biological features, which can’t be obtained directly by sequence information.

Hence, the second experiment is designed to compare the performance of standard AttCRISPR (hand-crafted biological features are used to improve performance of ensemble AttCRISPR) and current state-of-the-art method, DeepHF (the RNN mentioned above integrated with hand-crafted biological features).

3.2 Comparison to current methods

In order to make the comparison apples to apples, we follow Equation (15) to modify the ensemble method and design the control experiment using the same strategy to validate the conclusion that integrating with hand-crafted biological features can improve the predictive performance of methods. What’s more, we compare the standard AttCRISPR and current state-of-the-art method, DeepHF, and show the results in Table 3.

As shown in Table 3, in the absence of hand-crafted biological features, AttCRISPR has significant advantages over DeepHF in predictability. Further, integration with the hand-crafted biological features can also improve the performance of AttCRISPR, and achieve Spearman correlation coefficients of 0.872, 0.867 and 0.867 for WT-SpCas9, eSpCas9(1.1) and SpCas9-HF1 respectively. Meanwhile, current state-of-the-art method, DeepHF achieve 0.867, 0.862 and 0.860 respectively. After integrating with biological features, the performance gap between AttCRISPR and DeepHF is shortened, while AttCRISPR still has better performance. In addition, we also compare the standard deviation of data

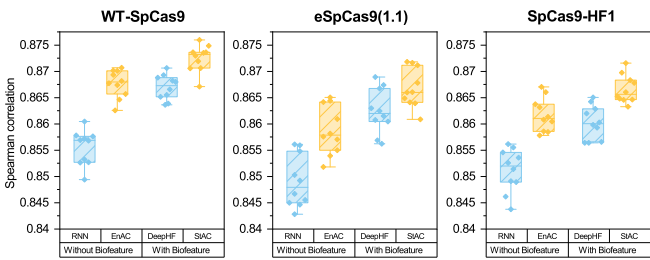


Fig. 7. Performance comparisons for methods before and after integrating with hand-crafted biological features, where DeepHF is the RNN integrated with hand-crafted biological features, and StAC is the EnAC integrated with hand-crafted biological features. The box plot show the mean and distribution of Spearman correlation coefficient between predicted and measured sgRNA activity scores over all tests.

obtained in ten tests, which are also shown in Table 3. It reveal that AttCRISPR is more stable than DeepHF.

3.3 Interpretability of the AttCRISPR

To some extent, the attention module in the AttCRISPR can help us to understand the decisions it makes. In the following sections, we will analyze the insight into activity of sgRNA bring through the attention mechanism at both global and local levels.

In the following content, when we use the word, global, we are referring to rules that are common throughout the data set. If assumed the method with strong generalization ability, it might mean that these rules is common in the corresponding Cas9 system. On the other hand, local refers to the rules applicable to a certain sgRNA. We believe that the local interpretability is very helpful in the design and optimization of sgRNA.

3.3.1 Global interpretability

At global level, a important question we want AttCRISPR to answer is which nucleotide it prefers at each position on the sequence. In fact, Wang *et al.* has already answered this question in detail with the DeepSHAP method. Leaving aside nucleotides, just consider the importance of each position, the method of Liu *et al.* have gone some way too. While our method is not based on the post hoc explanations techniques and input perturbations, the only work we need to do is to get the first-order preference  $A$  generated by the attention module. Specifically, we use the first-order preference  $A_s$  generated by the spatial attention module instead of  $\tilde{A}$  generated by the temporal attention module. The latter is in a higher dimensional dense space which make it difficult to understand. In practice, we input every sgRNA into the spatial AttCRISPR, in order to obtain the  $A_s$  from the spatial attention module and take its mean value. Then we rescale it through Z-score to obtain a standardization value and the final result is shown in Figure 8.

As shown in Figure 8, we captured the preference for each position-dependent nucleotide on the sgRNA sequence. The result revealed that A and G typically have a positive contribution to the activity of sgRNA, while T typically have a negative contribution. It is agree with the previous conclusion that when Cas9 is binding sgRNA, it prefer the one containing purines to pyrimidines (Wang *et al.*, 2014). In addition, global interpretability also pointed out that distinct from other nucleotides, G is strongly favored at position 20. This is consistent with the conclusions of several other reports (Wong *et al.*, 2015; Doench *et al.*, 2014).

Furthermore, the preference of the nucleotide at the same position doesn’t change dramatically with the Cas9 nucleases, while we still notice that compared with the other two datasets, C makes a more positive

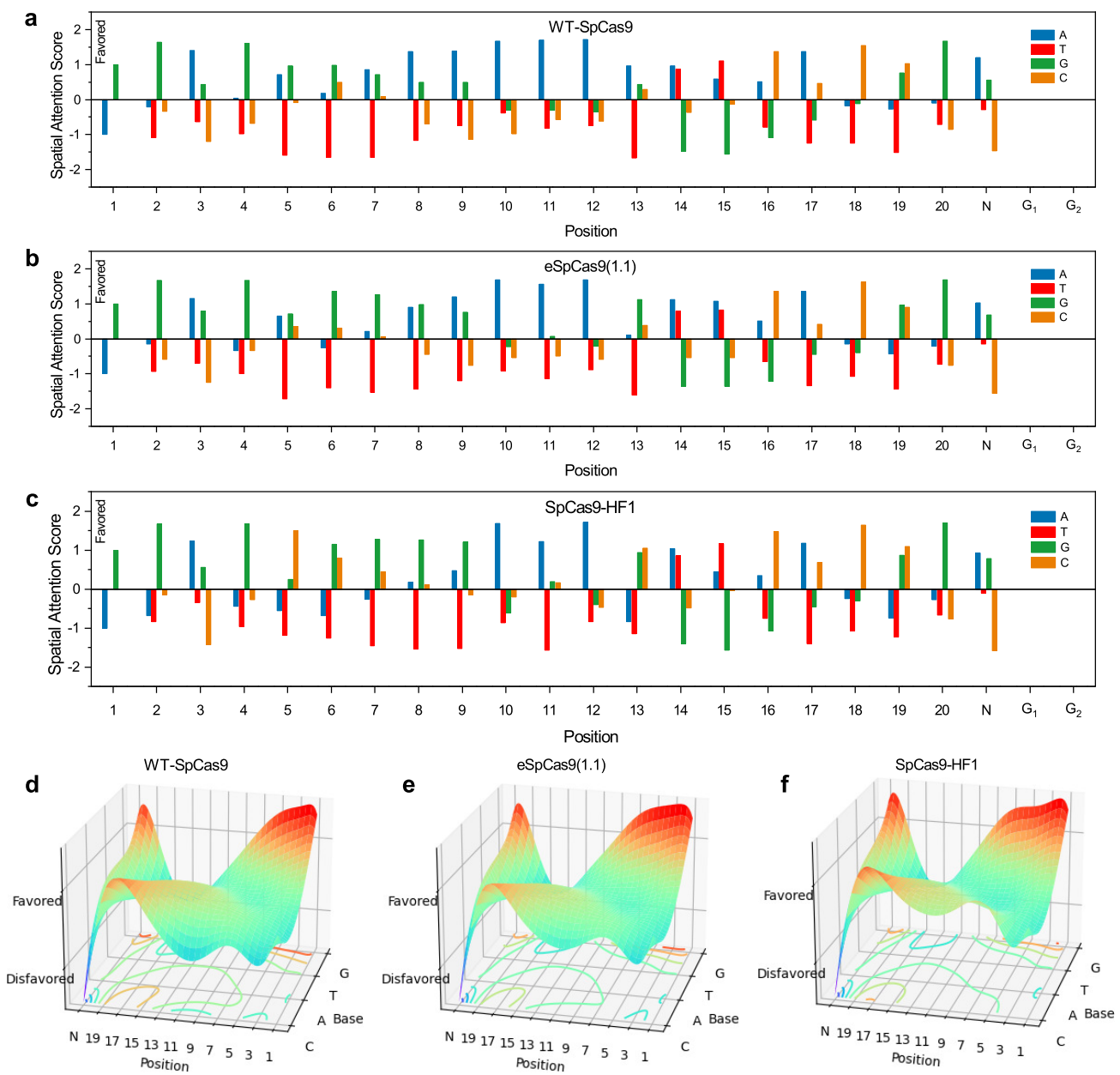


**Fig. 8.** Preference for each position-dependent nucleotide on the sgRNA sequence. (a)-(c) Bars show the score of preference after standardization, and the higher the number, the more positive it is for activity of sgRNA. The numbers below indicated the position of the nucleotides on-target DNA. (d)-(f) Preference surfaces for each position-dependent nucleotide fitted with Bézier surfaces. Each position-dependent nucleotide is a control point. The coordinates of the control points on the vertical axis represent the degree of preference, and the higher the position-dependent nucleotide corresponding to the control point is, the more positive it is for the activity of sgRNA. The contour plots at the bottom show the area of position-dependent nucleotides which have different contribution to the activity of sgRNA.

contribution to the activity of sgRNA with the SpCas9-HF1 especially in the position 5, which is evident in Figure 8 d-f.

The above discussion shows that, in the task of sgRNA activity prediction, attention mechanism can help us understand the decision made by AttCRISPR and reveal the insight into activity of sgRNA. Some of them are consistent with the conclusion accepted current.

3.3.2 Local interpretability

At local level, we will analyze a case (consisting of three sgRNAs as Table 4 show), then answer two important question based on the local

interpretability. First, how to optimize a sgRNA with local interpretability to make it have more on-target activity. Second, in the eyes of AttCRISPR, what are the reasons for the low activity of the sgRNA.

For the first question, we input the least-active sgRNA in Table 4 (with the index of 8493 and the activity of 0.831, call source sgRNA for convenience) into the temporal AttCRISPR. The score of each position is obtained based on Equation (7) (the calculated symbol with  $W$  is Hadamard product instead of dot product, in order to achieve the result in vector form), and the results are shown in Figure 9. According to Figure 9, scores at position 14 and 16 of source sgRNA are significantly below



Table 4. Three sgRNA and their activity

Index	sgRNA	Activity
8493	ACATGACTTTGGATTCCCCAGG	0.831
8492	ACATGACTTTGGATTCCCCAGG	0.869
8491	ACATGACTTTGGACTTCCCCAGG	0.861

Index represents its index in the source data (Supplementary Data 1), Activity represents its activity reported in WT-SpCas9 dataset.

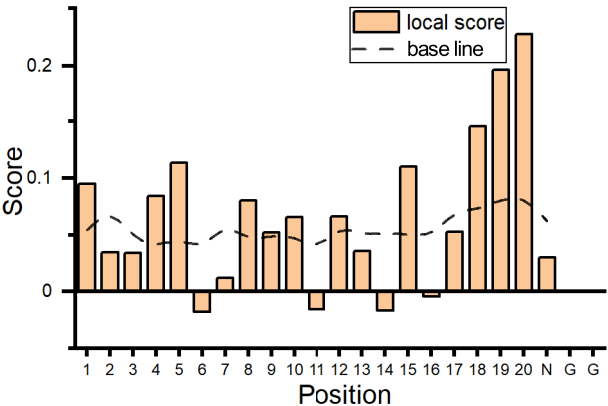


Fig. 9. The scores of sgRNA with index of 8493 obtained by the temporal AttCRISPR. The bar plot reveals the score at each position at local level, while the line of dashes reveals the scores at global level. At global level we calculated the scores of all sgRNA, then average the scores at each position to obtain the global level which can be used as base line and is helpful to judge the relative height of the scores.

the base line (in fact, the scores at position 6 and 11 is also noteworthy, however, we don't find sgRNA in the dataset for comparison). If replaced the T at position 14 with C, would generate the same sgRNA as the one with index of 8491, which is with a activity value of 0.861. If replaced the T at position 16 with C, would generate the same sgRNA as the one with index of 8492, which is with a activity value of 0.869. Therefore, we could conclude that the local interpretability is helpful for us to optimize the sgRNA without exhaustively search.

The second question we want AttCRISPR to answer is why it give two low scores at position 14 and 16. In practice, we will try to answer this question with second-order preference. Let AttCRISPR output the second-order preference matrix  $B$  corresponding to the source sgRNA, and show it in Figure 10. It is obvious that a few unusual bright spots appear in the red box in Figure 10. We believe that tells us the nucleotide at position 15 has a great effect on the score of position 14 and 16 (instead of position 13 or 17, which corresponding position are relatively dim in color). As shown in Table 4, in source sgRNA there are three consecutive Ts at position 14, 15 and 16, and this may reveal that multiple consecutive Us on sgRNA would leads to low on-target activity of sgRNA, which is consistent with earlier report (Wu *et al.*, 2014).

4 Discussion

In this article, we have introduced a new prediction methods, called AttCRISPR for the activity of sgRNA. For the first time, we take the ensemble of both spatial and temporal domain to predict the on-target activity of sgRNA. Throught ablation analysis and testing a series of possible network structure, we demonstrate that the ensemble method performs better than other methods on this task. In addition, we apply attention modules in both the spatial and temporal parts of AttCRISPR,

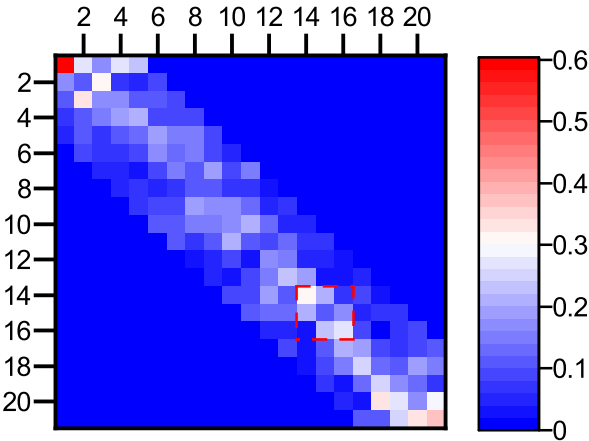


Fig. 10. The visualization of second-order preference matrix  $B$ , the elements in the  $i$ -th row and the  $j$ -th column represent the influence of nucleotide at position  $j$  when generate the first-order preference  $\tilde{A}$  at position  $i$ . The warmer the color, the more important it is. In the red box, a few unusual bright spots appear. To be more specific, the nucleotide at position 15 has a great effect on the first-order preference at positon 14 and 16.

and design two experiments combined with some early reports to prove that attention mechanisms can help researcher understand the decisions made by model which make it easy to optimize low activity sgRNA without exhaustively search.

In Section 3.1, we have tested both spatial and temporal domain AttCRISPR, and CNN (method in spatial domain), RNN (method in temporal domain) which reported by Wang *et al.* in the absence of hand-crafted biological features. A worth noticing point is that there is a gap between spatial AttCRISPR and CNN, though the performance of temporal AttCRISPR is basically the same as that of RNN. We suspect there are two possible reasons. One is that attention modules can significantly improve the performance of the model, which is short of experimental validation, and the other is the performance of the method in spatial domain is underestimated.

In Section 3.2, also integrating with hand-srafted biological features to improve the predictive performance, the performance gap between AttCRISPR and DeepHF is shortened, while AttCRISPR still has better performance. This may be a natural belief that with the primary biological sequence we can predict the functional and structural information. Therefore, there is a limit to the improvement of the performance by integrating with hand-srafted biological features.

In Figure 10 of Section 3.3.2, we note that the brightness at coordinates (14, 15) and (16, 15) exceeds (14, 13) and (16, 17). In other words, there are two unusual bright spots at coordinates (14, 15) and (16, 15). This could explain that the nucleotide trimer at position 14, 15, 16 has a great influence on the decision made by AttCRISPR. We believe that we can use a carefully designed  $3 \times 3$  convolution kernel, and move it along the diagonal of the second-order preference matrix  $B$ , in order to find all kind of nucleotide trimer that have a great influence on the decision made by AttCRISPR. However, due to the lack of validation method, we don't implement it in our work.

The current architecture of AttCRISPR focuses on predicting the on-target activity of conventional sgRNA which have a PAM based on NGG. However it can be extended to other Cas9 species, variants or off-target task easily.

## 5 Conclusion

In this paper, all the existing prediction method of sgRNA on-target activity are categorized as encoding-based spatial domain method and embedding-based temporal domain method, according to the processing method of input sgRNA. Then, we develop AttCRISPR, a ensemble method of both spatial method and temporal method follow the stacking strategy with strong interpretability. AttCRISPR prove that the ensemble method have a better performance in the datasets of DeepHF and can compete with the current state-of-the-art method. In addition, AttCRISPR apply attention mechanisms in both the temporal and spatial part, and we explain the decisions made by AttCRISPR through the attention module which is consistent with earlier reports. Further, we also point out that the output of the attention module can be used to optimize the low-activity sgRNA without exhaustively search, and our optimization results are verified with available experimental data. To our knowledge, this is the first time that the attentional mechanism is used to reveal the reasons influencing on-target activity of sgRNA, and assist sgRNA design.

## References

Chuai, G., Ma, H., Yan, J., Chen, M., Hong, N., Xue, D., Zhou, C., Zhu, C., Chen, K., Duan, B., et al. (2018). Deepcrispr : optimized crispr guide rna design by deep learning. *Genome Biology*, **19**(1), 1–18.

Cong, L., Ran, F. A., Cox, D. D., Lin, S., Barretto, R. P. J., Habib, N., Hsu, P., Wu, X., Jiang, W., Marraffini, L. A., et al. (2013). Multiplex genome engineering using crispr/cas systems. *Science*, **339**(6121), 819–823.

Doench, J. G., Hartenian, E., Graham, D. B., Tothova, Z., Hegde, M., Smith, I., Sullender, M., Ebert, B. L., Xavier, R. J., and Root, D. E. (2014). Rational design of highly active sgRNAs for crispr-cas9-mediated gene inactivation. *Nat. Biotechnol.*, **32**(12), 1262–1267.

Ishii, T. (2017). Reproductive medicine involving genome editing: clinical uncertainties and embryological needs. *Reproductive Biomedicine Online*, **34**(1), 27–31.

Jinek, M., Chylinski, K., Fonfara, I., Hauer, M., Doudna, J. A., and Charpentier, E. (2012). A programmable dual-rna-guided dna endonuclease in adaptive bacterial immunity. *Science*, **337**(6096), 816–821.

Kang, X., He, W., Huang, Y., Yu, Q., Chen, Y., Gao, X., Sun, X., and Fan, Y. (2016). Introducing precise genetic modifications into human 3pn embryos by crispr/cas-mediated genome editing. *Journal of Assisted Reproduction and Genetics*, **33**(5), 581–588.

Kim, H. K., Min, S., Song, M., Jung, S., Choi, J. W., Kim, Y., Lee, S., Yoon, S., and Kim, H. (2018). Deep learning improves prediction of crispr-cpf1 guide rna activity. *Nat. Biotechnol.*, **36**(3), 239–241.

Kim, H. K., Kim, Y., Lee, S., Min, S., Bae, J. Y., Choi, J. W., Park, J., Jung, D., Yoon, S., and Kim, H. H. (2019). Spcas9 activity prediction by deepspcas9, a deep learning-based model with high generalization performance. *Sci. Adv.*, **5**(11).

Kleinstiver, B. P., Pattanayak, V., Prew, M. S., Tsai, S. Q., Nguyen, N. T., Zheng, Z., and Joung, J. K. (2016). High-fidelity crispr-cas9 nucleases with no detectable genome-wide off-target effects. *Nature*, **529**(7587), 490–495.

Liang, P., Xu, Y., Zhang, X., Ding, C., Huang, R., Zhang, Z., Lv, J., Xie, X., Chen, Y., Li, Y., et al. (2015). Crispr/cas9-mediated gene editing in human triploid zygotes. *Protein & Cell*, **6**(5), 363–372.

Lin, J. and Wong, K.-C. (2018). Off-target predictions in CRISPR-Cas9 gene editing using deep learning. *Bioinformatics*, **34**(17), i656–i663.

Liu, G., Zhang, Y., and Zhang, T. (2019a). Computational approaches for effective crispr guide rna design and evaluation. *Computational and structural biotechnology journal*, **18**, 35–44.

Liu, Q., He, D., and Xie, L. (2019b). Prediction of off-target specificity and cell-specific fitness of crispr-cas system using attention boosted deep learning and network-based gene feature. *PLoS computational biology*, **15**(10), e1007480–e1007480.

Liu, Q., Cheng, X., Liu, G., Li, B., and Liu, X. (2020). Deep learning improves the ability of sgRNA off-target propensity prediction. *BMC Bioinformatics*, **21**(1), 51.

Luong, M.-T., Pham, H., and Manning, C. D. (2015). Effective Approaches to Attention-based Neural Machine Translation. *arXiv e-prints*, page arXiv:1508.04025.

Mali, P., Yang, L., Esvelt, K. M., Aach, J., Guell, M., Dicarlo, J. E., Norville, J. E., and Church, G. M. (2013). Rna-guided human genome engineering via cas9. *Science*, **339**(6121), 823–826.

Muhammad Rafid, A. H., Toufikuzzaman, M., Rahman, M. S., and Rahman, M. S. (2020). Crisprpred(seq): a sequence-based method for sgRNA on target activity prediction using traditional machine learning. *BMC Bioinformatics*, **21**(1), 223.

Rubeis, G. and Steger, F. (2018). Risks and benefits of human germline genome editing: An ethical analysis. *Asian Bioethics Review*, **10**(2), 133–141.

Slaymaker, I. M., Gao, L., Zetsche, B., Scott, D. A., Yan, W. X., and Zhang, F. (2016). Rationally engineered cas9 nucleases with improved specificity. *Science*, **351**(6268), 84–88.

Song, M., Kim, H. K., Lee, S., Kim, Y., Seo, S.-Y., Park, J., Choi, J. W., Jang, H., Shin, J. H., Min, S., Quan, Z., Kim, J. H., Kang, H. C., Yoon, S., and Kim, H. H. (2020). Sequence-specific prediction of the efficiencies of adenine and cytosine base editors. *Nat. Biotechnol.*, **38**(9), 1037–1043.

Vaswani, A., Shazeer, N., Parmar, N., Uszkoreit, J., Jones, L., Gomez, A. N., Kaiser, L., and Polosukhin, I. (2017). Attention Is All You Need. *arXiv e-prints*, page arXiv:1706.03762.

Wang, D., Zhang, C., Wang, B., Li, B., Wang, Q., Liu, D., Wang, H., Zhou, Y., Shi, L., Lan, F., et al. (2019). Optimized crispr guide rna design for two high-fidelity cas9 variants by deep learning. *Nat. Communications*, **10**(1), 4284–4284.

Wang, S., Peng, J., Ma, J., and Xu, J. (2016). Protein secondary structure prediction using deep convolutional neural fields. *Sci. Rep.*, **6**(1), 18962.

Wang, T., Wei, J. J., Sabatini, D. M., and Lander, E. S. (2014). Genetic screens in human cells using the crispr/cas9 system. *Science*, **343**(6166), 80–84.

Wong, N., Liu, W., and Wang, X. (2015). Wu-crispr: characteristics of functional guide RNAs for the crispr/cas9 system. *Genome Biology*, **16**(1), 218.

Woo, S., Park, J., Lee, J., and Kweon, I. S. (2018). CBAM: convolutional block attention module. In V. Ferrari, M. Hebert, C. Sminchisescu, and Y. Weiss, editors, *Proceedings of the European Conference on Computer Vision (ECCV) 2018*, volume 11211 of *Lecture Notes in Computer Science*, pages 3–19. Springer.

Wu, X., Scott, D. A., Kriz, A. J., Chiu, A. C., Hsu, P., Dadon, D. B., Cheng, A. W., Trevino, A. E., Konermann, S., Chen, S., et al. (2014). Genome-wide binding of the crispr endonuclease cas9 in mammalian cells. *Nat. Biotechnol.*, **32**(7), 670–676.

Zhang, G., Dai, Z., and Dai, X. (2020). C-rnn-crispr: Prediction of crispr/cas9 sgRNA activity using convolutional and recurrent neural networks. *Computational and structural biotechnology journal*, **18**, 344–354.